Applied Catalysis B: Environmental 299 (2021) 120706

Contents lists available at ScienceDirect

Applied Catalysis B: Environmental

journal homepage: www.elsevier.com/locate/apcatb

UV/H_2O_2 degradation of diclofenac in a photocatalytic fuel cell

Rebecca Dhawle, Dionissios Mantzavinos *, Panagiotis Lianos *

Department of Chemical Engineering, University of Patras, 26500 Patras, Greece

ARTICLE INFO

Keywords:
Diclofenac
Photocatalytic fuel cell
PFC
UV/H_2O_2

ABSTRACT

The purpose of this work was to construct an integrated reactor which could photoelectrocatalytically generate hydrogen peroxide under solar radiation and simultaneously degrade a recalcitrant pollutant by the UV/H_2O_2 process. Diclofenac has been chosen as water soluble model pollutant. Hydrogen peroxide has been produced by atmospheric oxygen reduction in a photocatalytic fuel cell. The cell comprised a transparent photoanode electrode bearing a combined CdS/TiO_2 photocatalyst and a carbon cloth cathode bearing nanoparticulate carbon without any other electrocatalyst. Diclofenac was dissolved in the cathode compartment where hydrogen peroxide was generated and the pollutant was degraded by UV radiation support. Degradation was monitored by UV–Vis spectrophotometry and by high performance liquid chromatography. The results show that an integrated reactor functionality is realistic and effective and it provides an alternative route for sustainable operation aiming at environmental remediation.

1. Introduction

Use of solar radiation for environmental remediation purposes is a very attractive prospect which has created several new research fields. Modern life and extensive urbanization have led to the introduction of organic pollutants into ground waters. Many of these pollutants are recalcitrant and they cannot be biologically degraded; therefore, advanced oxidation processes (AOP) are necessary in order to mineralize these water contaminants and thus clean polluted water. One such powerful AOP is a combination of UV radiation with H_2O_2 (UV/H_2O_2) [1–10]. UV radiation may photolyze the organic substance by itself; however, UV most effectively dissociates H_2O_2 leading to the formation of highly oxidative radicals which interact with organic pollutants and mineralize them. The present work studies such a process and seeks for means of creating an integrated model device, capable of producing H_2O_2 by a sustainable solar process and of employing this product for the degradation of a recalcitrant organic pollutant. Diclofenac (DCF), a widely used non-steroid anti-inflammatory drug, was chosen as the target pollutant.

H_2O_2 has been photoelectrochemically produced by O_2 reduction in a photocatalytic fuel cell (PFC) [11–20]. The device employed is schematically illustrated in Fig. 1. It was an H-shaped reactor composed of two compartments separated by a silica frit acting as ion-transfer membrane. On the left side, was the photoanode electrode and on the right side the cathode electrode. Both electrodes were immerged in the respective electrolytes. The photoanode was made of a transparent electrode on which a combination of nanoparticulate semiconductor photocatalysts were deposited. The cathode was made of carbon cloth on which nanoparticulate carbon (carbon black) was deposited. Upon illumination, the photoanode absorbs photons generating electron and holes. Holes are consumed in oxidation reactions while electrons move through an external circuit and go to the cathode electrode where they assist reduction reactions. In the present work, mesoporous titania combined with CdS sensitizer has been used as a standard photocatalyst. The anode electrolyte contained NaOH and ethanol, the latter used as fuel which is oxidized acting as hole scavenger. This combination has been repeatedly used in the past and it is a very good model system for the construction of a PFC device [11–13,17]. At the cathode electrode, O_2 from air is reduced leading to hydrogen peroxide production [13,17]:

$$O_2 + 2H^+ + 2e^- \rightarrow H_2O_2 \ (+0.68 \text{ V vs. NHE}) \quad (1)$$

This 2-electron reduction scheme is more probable in the absence of a powerful electrocatalyst as is the present case, where only carbon black on carbon cloth has been used to make the cathode electrode. This assumption was justified by the experiment. Since the titania conduction band is the receiver of all photogenerated electrons, its level practically defines the potential of the anode electrode, which is located at about − 0.2 V vs. NHE. Therefore, there is enough self-bias to run the cell, i.e. anode potential (− 0.2 V) is substantially more negative than cathode potential (+ 0.68 V); therefore, the presently proposed cell can run as a

* Corresponding authors.
E-mail addresses: mantzavinos@chemeng.upatras.gr (D. Mantzavinos), lianos@upatras.gr (P. Lianos).

https://doi.org/10.1016/j.apcatb.2021.120706
Received 28 May 2021; Received in revised form 3 September 2021; Accepted 6 September 2021
Available online 11 September 2021

pure PFC just by shining light on the photoanode. As a matter of fact and as it will be also discussed later, the electrolyte of the cathode compartment contained Na_2SO_4 and the pH was around 6. Since the pH of the alkaline electrolyte of the anode compartment was around 12, the above cell additionally provided a chemical forward bias further assisting device functionality.

The cathode compartment in the device of Fig. 1 played a dual role. The target pollutant was dissolved into the electrolyte of the cathode compartment and was degraded in situ by the combined action of the photoelectrocatalytically produced H_2O_2 and the irradiation from a separate UV source. Therefore in the same compartment, H_2O_2 was produced and the pollutant was degraded. In order to separate the role of the photoanode excitation light source from the UV source used for degradation, the cathode compartment was shielded with the help of an appropriate cover, as illustrated in the Fig. 1. The photoanode excitation source may simply be natural solar light while the fuel may be any biomass derived organic waste [21,22]. Therefore, production of H_2O_2 is a sustainable process based on renewable resources. Apart from the need for a UV source, the proposed device is an integrated model system that can employ solar radiation to degrade pollutants.

As already said, the target pollutant in the present case was DCF. Because of its wide use, ground water may be heavily loaded with DCF. This drug is recalcitrant and very harmful to the environment [23–25]. It is not then a surprise that its degradation by various procedures has been extensively studied [26–35]. This is why DCF was chosen as a model water contaminant to perform the present measurements. Our purpose was not to study DCF degradation per se but to use its degradation as model to evaluate the presently proposed device and procedures. The main target of the present work is then to demonstrate the feasibility of the construction of an integrated system that can produce H_2O_2 by exploiting solar radiation, simultaneously degrade a recalcitrant pollutant by UV/H_2O_2 and delimit the possibilities of on line monitoring of degradation. Unlike our recently published work [17] that showcased the concept of photocatalytic fuel cell in model, dye-containing solutions, the environmental significance and applicability are demonstrated in this study. This is done by working with environmentally relevant (i) samples (e.g. wastewater and seawater) beyond pure water, and (ii) contaminant concentrations at the low μg/L level. Such specifications may allow the construction of a portable device for both degradation and detection.

2. Experimental

2.1. Materials

Unless otherwise specified, all reagents were obtained from Sigma-Aldrich and were used as received. Fluorine-doped Tin Oxide electrodes (FTO, 8 ohm/square) were purchased from Pilkington (USA), carbon cloth (CC) from Fuel Cell Earth (Wobum, MA, USA), carbon black (CB) from Cabot Corporation (Vulcan XC72, Billerica, MA, USA) and Silica frit from ROBU (ROBU Glasfilter-Geräte GmbH, Hattert, Germany).

2.2. Description of the reactor

The device used to carry out the present measurements was a home-made H-shaped reactor built of Pyrex glass. It was composed of two compartments separated by an ion-transfer membrane, which in the present case was a silica frit (ROBU VitraPOR Quartz filter disc, Por. SGQ5, diameter 25 mm, thickness 2 mm, amorphous porous silica). The device is schematically illustrated by Fig. 1. The left side represents the photoanode and the right side the cathode compartment. The active volume of each compartment was 150 ml. They were both filled with electrolytes. The electrolyte of the photoanode compartment was in all cases 0.5 M aqueous NaOH to which we added 5% v/v EtOH, playing the role of fuel to run the cell. The aqueous electrolyte of the cathode compartment contained Na_2SO_4 at various concentrations and DCF. For the latter, the concentration was 20 μM for UV–Vis and 2 μM for HPLC (high performance liquid chromatography) measurements. As already said, with these electrolytes the pH in the photoanode compartment was approximately 12 and in the cathode compartment approximately 6. Alternatively, the cathode compartment was filled with either natural sea water or with common bottle water or municipal wastewater. Sea water did not necessitate any electrolyte but addition of Na_2SO_4 was necessary in the case of bottle and municipal wastewater. In the latter cases the pH was adjusted to 6. The pH of the sea water was 4.5 and it was left as it was. The photoanode electrode (left) and the cathode electrode (right) were dipped in the respective electrolytes. The presence of the salt, when applicable, was necessary to run the photoelectrochemical cell and did not affect DCF degradation, as it will be actually shown by the present data. The composition of the bottle water and the presently used municipal wastewater is listed in the Supporting information file. Illumination of the photoanode and the cathode electrolyte was made by separate light sources with radiation passing through the pyrex glass. A Xe lamp was used for excitation of the

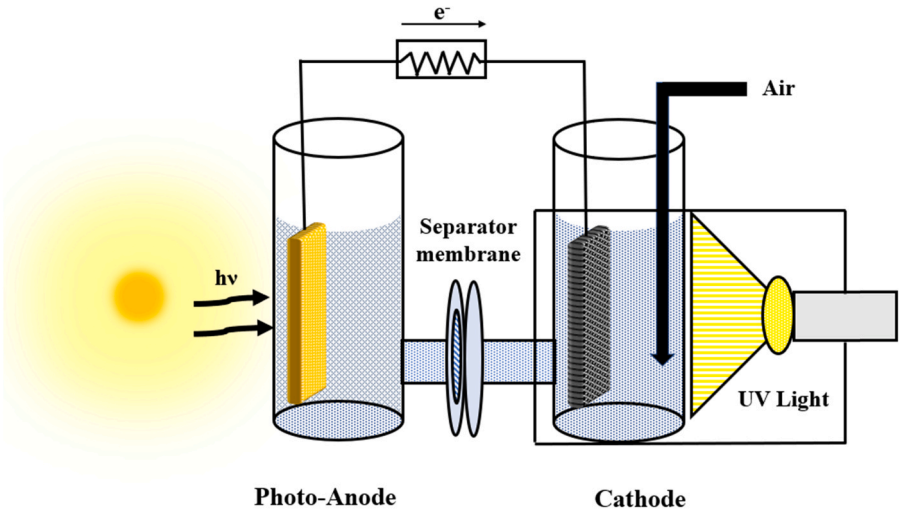

Fig. 1. Schematic illustration of the presently employed device.

photoanode providing about 100 mW cm^{-2} light intensity at the position of the photocatalyst. This is a rough simulation of solar radiation. The cathode compartment was surrounded by a cover that prevented any interference from the Xe lamp, which excited the photoanode. However, the cover had an opening which allowed illumination of the cathode compartment with a separate UV lamp. For this purpose an Osram SUPRATEC 400 W lamp peaking at 380 nm was used. The radiant flux provided by this lamp was measured by actinometry as detailed in the Supporting information file and was equal to 0.71 W. The corresponding radiant flux expressed in Ein s^{-1} was 2.25 μmol s^{-1}. The irradiated cross sectional area was 26.9 cm^2; therefore, the corresponding power densities were 263.4 W m^{-2} and 837.1 μmol m^{-2} s^{-1}, respectively.

2.3. Construction of the photoanode and cathode electrodes

The photoanode electrode was an FTO glass covered on the conductive side with a layer of titania carrying CdS as visible light sensitizer (CdS/TiO_2/FTO). The cathode electrode was a carbon cloth carrying on one side carbon black (CB/CC) without any added electrocatalyst. A standard procedure was used to make these electrodes, repeatedly published in the past [12,13,17]. Briefly, to make the CdS/TiO_2/FTO photoanode electrode, a thin compact titania layer was first deposited on a patterned FTO electrode, followed by a thick layer of mesoporous titania of about 10 μm thickness, both calcined at 550 °C. Finally, CdS was synthesized within the titania mesopores by Successive Ionic Layer Adsorption and Reaction using $Cd(NO_3)_2$ and Na_2S as precursors. In turn, the CB/CC electrode was deposited on carbon cloth using a paste made of carbon black and a binder and was annealed at 340 °C.

2.4. DCF degradation procedure

Degradation of DCF was monitored in square 1 cm cuvettes by using absorbance spectrophotometry. Samples were collected from the cathode compartment and after measurement they were poured back into the electrolyte. Measures were taken to control any adsorption of the drug on the device components, which would affect drug quantity in solution. It was indeed found that materials like Nafion membrane are strong DCF adsorbers. This is a reason that the use of such a membrane was avoided. Adsorption of DCF was not detected on the silica membrane and adsorption on the counter electrode was negligible. Illumination of the anode compartment by the Xe lamp and the cathode compartment by the UV lamp was made separately but simultaneously. Degradation was also monitored by High Performance Liquid Chromatography (HPLC). 1.2 ml samples were collected at regular time intervals from the reactor. 0.3 ml of methanol was added to each sample to quench the reaction. Then the samples were filtered using a 0.2 μm (PVDF-Whatman) syringe to filter out any solid particles and were introduced in the device for measurement. As already said, DCF concentration was 20 μM for the UV–Vis and 2 μM for the HPLC measurements.

2.5. Measurements

Absorbance measurements were made with the help of a Cary 1E UV–Vis spectrophotometer (Houston, TX, USA) and current-voltage measurements with an Autolab potentiostat PGSTAT128N (Utrecht, The Netherlands). HPLC (Waters Alliance 2695) was used to analyze the concentration of Diclofenac. Separation was achieved on a Kinetex XB-C18 100A column [2.6 μm inner diameter 2.1 mm × 50 mm] and a 0.5 μm inline filter (KrudKatcher Ultra) both purchased from Phenomenex. The mobile phase consisted of 50:50 UPW:acetonitrile. The injection volume was 100 μL, whereas the detection was achieved through a UV-visible detector (Waters 2996) set at 275 nm. The quantity of the photoelectrochemically produced by O_2 reduction H_2O_2 was measured by a standard procedure based on potassium titanium (IV) oxalate (PTO) titration. The procedure is detailed in our previous publication [17].

3. Results and discussion

3.1. Monitoring DCF degradation by UV–Vis absorbance spectrophotometry

UV–Vis identification of an organic substance is a straightforward and facile method to monitor the presence of a pollutant and it can be easily done in situ. For a portable device, for example, UV–Vis spectrophotometry is also a low cost detection technique. For this reason, the applicability of such a method has been studied first, while an effort has been made to delimit its capacities.

The degradation of DCF has been repeatedly studied in the past and the degradation fragments have been identified by liquid chromatography and other techniques [26–35]. What is of interest in our case is the fact that DCF is photolyzed under UV irradiation even in the absence of any catalyst. Photolysis results in a dramatic change of its UV–Vis spectrum. This is important, in order to interpret the spectra of DCF during degradation. In most cases of studied pollutants, photocatalytic degradation leads to a progressive decrease of light absorbance while in the case of DCF a blow up of the UV–Vis spectrum is first observed, as it will be also shown in the present work. Indeed, an aqueous solution of 100 μM DCF was subjected to UV irradiation for several minutes and the effect on its UV–Vis spectrum was monitored and is shown in Fig. 2A. Curve 1 shows DCF spectrum before and Curve 2 after irradiation. The spectral expansion was even more dramatic in the presence of H_2O_2, as seen in Fig. 2B. The broad expansion of light absorbance into the Visible resulted to coloring of an original colorless solution. The absorbance maximum was reached after 30 min of irradiation and then a progressive decrease of absorbance was detected over the whole spectral range of measurement. Based on literature results, the dominant chemical structure transformations of DCF during photolysis are illustrated by

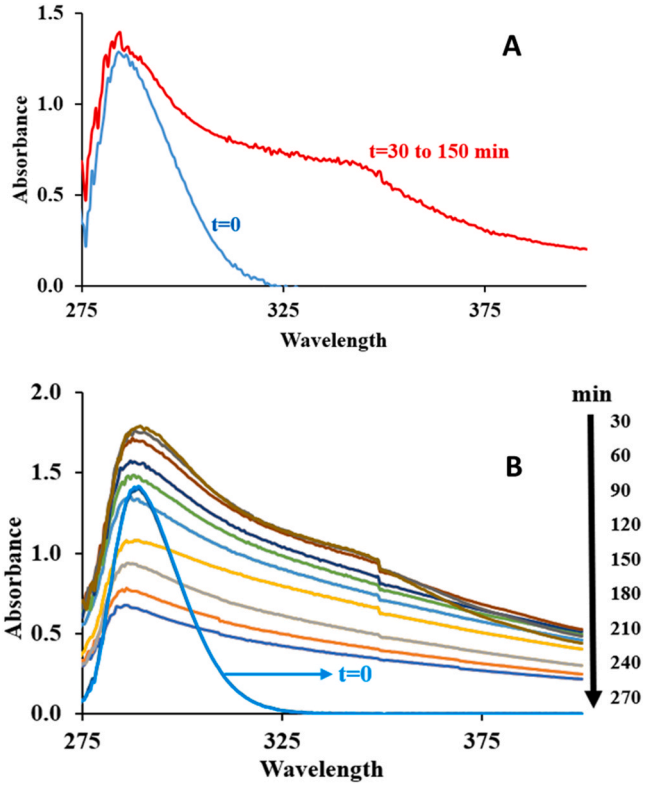

Fig. 2. Effect of UV irradiation on the absorbance spectra of aqueous solutions of 100 μM DCF in the absence (A) and in the presence (B) of 100 mg L^{-1} H_2O_2.

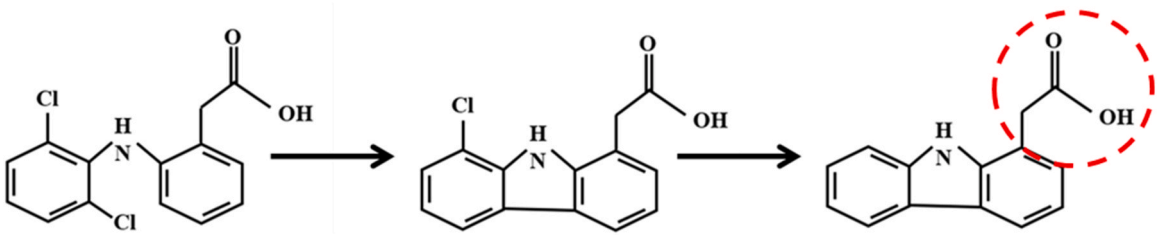

Fig. 3. Dominant transformations of DCF during photolysis include dechlorination and the loss of the carboxylic group. Loss of the second chlorine atom may be preceded by loss of the carboxylic group.

Fig. 3 [26–31,34,36]. Apparently, chlorine and carboxylic group extraction makes the first degradation steps. The spectra of Fig. 2 were obtained by using pure aqueous solutions. Sodium sulfate added to the aqueous solution in order to fit the electrolyte used to run the photoelectrochemical cell did not affect data.

UV irradiation of the sample beyond spectral expansion resulted into a uniform progressive decrease of absorbance over the whole spectral range. This degradation was observed only in the presence of H_2O_2 under the present conditions. In Fig. 2B, it is seen that DCF degradation is rather slow; however, this is a case of a very high DCF concentration (100 μM) and a rather limited H_2O_2 concentration (100 mg L^{-1}). This concentration of the drug was chosen in order to obtain a representative absorbance spectrum while the concentration of H_2O_2 was chosen to be within the range of photoelectrochemical H_2O_2 production by dioxygen reduction and by using the above described reactor. In fact, photoelectrochemical experiments were done with less concentrated DCF solutions (20 and 2 μM, cf. Section 2.4), the first one still detectable by absorbance spectrophotometry and the second by HPLC. Such concentrations, especially the first, are higher than the concentration of DCF found in real polluted waters [37] or much higher than the set European standards [38]. In other words, the data of the present work deal with most unfavorable conditions of heavily polluted waters. The UV/H_2O_2 degradation of a 20 μM aqueous DCF solution in the presence of 100 mg L^{-1} H_2O_2 is represented by the spectra of Fig. 4. In that case, the absorbance of DCF progressively went to zero. It is interesting to note that the absorbance maximum was then already low, obviously, because the ratio of H_2O_2/DCF concentration was in that case higher; therefore, the degradation was faster.

The above data provide a guide for monitoring DCF UV/H_2O_2 degradation by UV–Vis spectrophotometry in the case of the photoelectrochemical (PFC) device. The characteristics of the device operation are presented in the following sub-section.

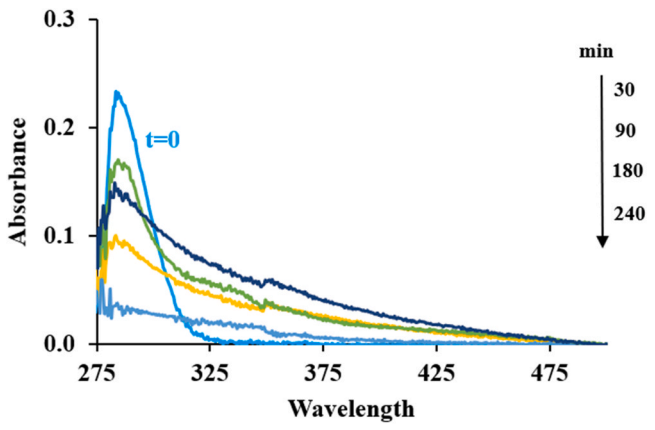

Fig. 4. Effect of UV irradiation on the absorbance spectra of aqueous solutions of 20 μM DCF in the presence of 100 mg L^{-1} H_2O_2.

3.2. Current-voltage characteristics of the photoelectrochemical reactor

The reactor of Fig. 1 has been used to produce hydrogen peroxide and degrade DCF under the effect of combined UV/H_2O_2 oxidation. The current-voltage characteristics of this reactor are shown in Fig. 5. The curve was drawn in the light-chopping mode to clearly show the range of pure photocurrent, which was between − 0.5 and 1.0 V. Above 1.0 V, part of the current is due to electrolysis. This is why dark current did not become zero at V > 1 V. The curve was drawn in a 2-electrode configuration, i.e., with a photoanode and a counter electrode, without reference electrode. The fact that photocurrent was produced at short-circuit conditions, i.e. at V = 0 V, shows that the device functions as photocatalytic fuel cell producing electricity just by shining light on the photoanode. No bias is necessary to run the photoelectrochemical cell. However, when necessary and in order to increase current, a forward (anodic) bias may be applied. Photogenerated electrons moved from the photoanode to the counter electron where they produced H_2O_2 by oxygen reduction. An air-saturated electrolyte was used to assure O_2 supply. The rate of H_2O_2 production by the present reactor is presented in the next subsection.

3.3. Monitoring the photoelectrochemical production of hydrogen peroxide

The photoelectrochemical production of H_2O_2 has been monitored at a current flow of 13.4 mA (short circuit current). The quantity of H_2O_2 was determined by titration with PTO, as already said. Fig. 6 shows two curves. A model curve based on Eq. (1), showing the expected quantity of H_2O_2 under ideal conditions of 100% efficiency and the actual experimental curve. The model curve (1) assumes that 1 H_2O_2 molecule is produced for every 2 electrons arriving at the counter electrode. Consequently, *1 μmole min^{-1} of a substance which is formed by 2 electrons per molecule, corresponds to 10^{-6} (moles) × 6.023 × 10^{23} (molecules $mole^{-1}$) × 2 × 1.602 × 10^{-19} (C $molecule^{-1}$) × (60 s^{-1}) = 3.21 mA.*

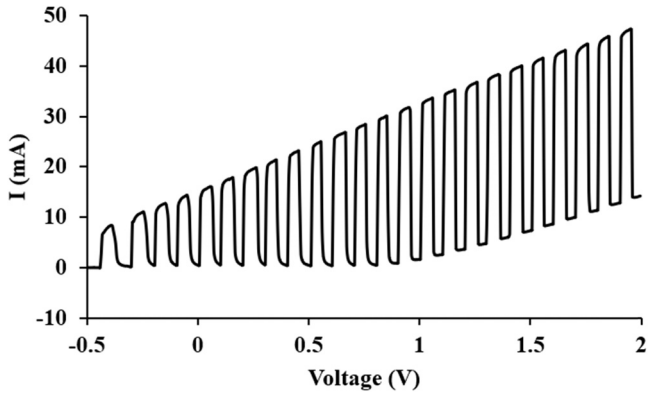

Fig. 5. Current-voltage characteristics of the presently employed H-shaped reactor recorded in the light-chopping mode. The curve shows that pure photocurrent may be produced in the range between − 0.5 and 1.0 V. Above 1.0 V, part of the current is due to electrolysis.

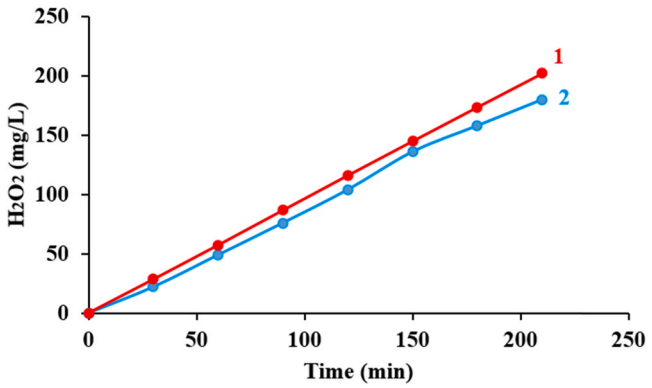

Fig. 6. Theoretical (1) and experimental (2) quantity of H_2O_2 produced by the presently used reactor and by cathodic dioxygen reduction as a function of time.

Thus, the rate R (moles min^{-1}) of H_2O_2 expected to be produced is found by dividing current by 3.21. Finally, the corresponding quantity of H_2O_2 expressed in mg/L was calculated by the formula: $C(g/L) = R\ (moles\ min^{-1}) \times 10^{-6} \times 34 \times 10^{3}\ (mg\ mole^{-1}) \times t\ (min) \times 6.67\ (L^{-1})$. 34,000 mg $mole^{-1}$ corresponds to the molecular weight of H_2O_2, t is the duration of the measurement in min and 6.67 is the number of times one needs to multiply the volume of the cathode compartment (150 ml) to make a liter. Thus the ideal curve was built as a function of time. The second curve (2) showing the corresponding experimental values revealed a very efficient system with experimental values very close to the theoretical ones, approaching 100% Faradaic efficiency. Hydrogen peroxide was continuously produced since the first few minutes of device operation. In view of the data of Section 3.1, it is now certified that the presently used reactor can produce sufficient quantity of H_2O_2 to carry out degradation of DCF. This stage is analyzed in the following subsection.

3.4. Degradation of DCF by combined H_2O_2 production and UV irradiance

The reactor of Fig. 1 has been used both for the production of H_2O_2, as already said, and for the degradation of DCF. DCF was introduced in the electrolyte of the cathode compartment at a concentration of 20 μM. The cathode compartment was surrounded by a cover which prevented interference by the source exciting the photoanode and carried an opening for the introduction of the UV light from a separate source. As already said, the radiant flux was around 0.71 W (see Section 2.2). Under these conditions, a progressive modification of the UV–Vis absorbance of the dissolved drug was observed, as presented in Fig. 7. The inset of Fig. 7 shows the absorbance maximum also as a function of time. Some interesting features can be distinguished in these data. The absorbance spectrum was first expanded into the Visible and the absorbance maximum first increased. Then the absorbance decreased over the whole absorbance spectrum. The absorbance maximum first increased fast, then there was a slow decrease and finally a rather fast decrease. Spectral modification was in line with the data of Figs. 2–4. DFC was first rapidly photolyzed and because the quantity of hydrogen peroxide was small at the beginning but built up in the course of time the degradation was first slow and later was accelerated, as shows the inset of Fig. 7.

The above data show that DCF degradation is indeed possible by the above combined procedure where H_2O_2 can be produced photoelectrocatalytically and can degrade the pollutant with the assistance of UV radiation. The concentration of DCF introduced into the above reactor was 20 μM, which is relatively high, as compared to the usual DCF loads in ground waters [37]. Therefore, the above procedure was applied under hard conditions of heavily polluted water. Things become easier if the pollutant load is smaller, even though, in that case degradation cannot be accurately monitored by UV–Vis spectrophotometry. In that case, it was necessary to employ a more sensitive technique and as such we have used HPLC. The degradation of 2 μM DCF is shown in Fig. 8 (curve 1). Any traces of DCF vanished after 50 min of device operation while the data of Fig. 7 shows that several hours are necessary for the same effect if more concentrated samples are used.

However, in Fig. 8 there is a second curve showing decay just by UV radiation in the absence of H_2O_2 and in the absence of electrolyte. It is seen that the two curves are almost identical at short times and evolve apart at later times. In fact, most of the decay of DCF is done at short times and it is obviously due to photolysis. HPLC detects the intact DCF molecules and as such carries a disadvantage compared to other detection techniques. In this respect, UV–Vis absorbance spectrophotometry is to a certain extent capable of demonstrating the degradation stage by highlighting the photolysis step. On the other hand, UV–Vis spectrophotometry is limited to relatively high concentrations of the pollutant. The above information is then useful in order to delimit the possibilities of both techniques.

The proposed integrated reactor may be restricted by the fact that it necessitates the presence of an electrolyte. Photoelectrochemical H_2O_2 production rate depends on the electric current flowing across the electrodes and current depends on electrolyte conductivity. Of course, conductivity is higher when electrolyte concentration is higher. In the above cell the electrolyte in the photoanode compartment was kept always the same. On the contrary, the electrolyte in the cathode compartment was modified in terms of salt concentration. Thus Na_2SO_4

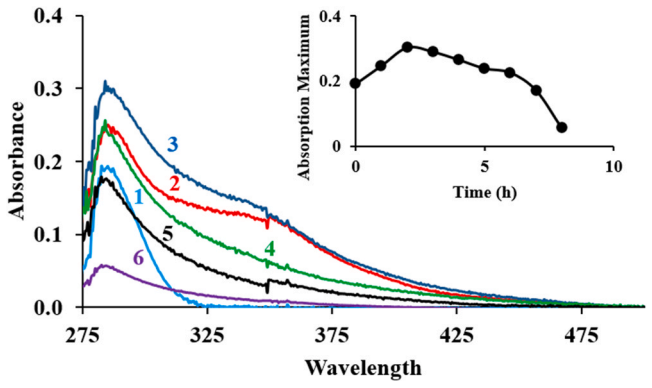

Fig. 7. Progressive variation of the UV–Vis absorbance spectra of 20 μM DCF dissolved in 0.5 M aqueous Na_2SO_4 in the cathode compartment of the PFC as a function of time (hours): (1) 0; (2) 1; (3)2; (4)6; (5) 7; and (6) 8. Inset: absorbance maximum vs. time.

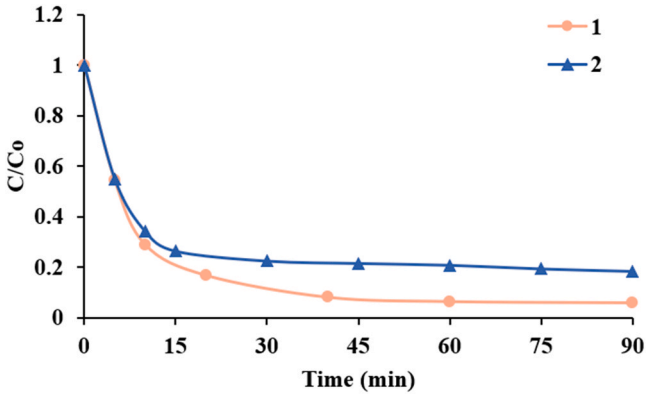

Fig. 8. UV radiation decay of the relative concentration of 2 μM DCF as a function of time monitored by HPLC: (1) dissolved in 0.5 M aqueous Na_2SO_4 in the cathode compartment of the PFC where H_2O_2 is photoelectrocatalytically produced and (2) dissolved in pure water without additives.

concentration was changed in the range of 0.05–0.5 M and the effect on DCF degradation was studied by HPLC. The results are shown in Fig. 9. The three curves obtained at three different salt concentrations were practically the same, demonstrating that the concentration of the salt did not have any detectable influence on DCF degradation. The above variation of the salt concentration did affect current but to a rather limited extent. The corresponding currents at short-circuit conditions (zero bias) were 12.7, 13.0 and 13.4 mA. This is a relatively small current variation and it is explained by the fact that the concentration of NaOH and that of the fuel in the anode compartment remained the same; therefore, the supply of photogenerated electrons did not substantially change. Consequently, the production of H_2O_2 did not substantially change either. Hence, the absence of any salt concentration affect. One may then deal with conductivity and H_2O_2 production rate issues by taking into account pollutant concentration and H_2O_2 demand, in order to achieve efficient degradation.

In order to highlight the possibilities of practical applications for the present system, degradation of DCF has been studied in common bottle water, in municipal wastewater and in natural sea water. In the case of bottle water and municipal wastewater, it was necessary to add 0.1 M Na_2SO_4 in order to run the cell. No electrolyte was necessary in the case of sea water. Indeed, the conductivity of the Na_2SO_4 electrolyte at the presently employed salt concentrations is compatible [39] with that of sea water (conductivity of sea water ranges between 30 and 60 mS/cm). In all three cases, 2 μM of DCF was added and the samples were introduced in the cathode compartment of the PFC. The current-voltage characteristics of the cell were similar in all cases. As an example, the case of sea water is shown in Fig. S1 of the Supporting Information file. The degradation was monitored by HPLC. Fig. 10 shows the obtained results in comparison with corresponding results of the pure-water-containing sample. The degradation followed a similar trend with all four samples. Small differences may be related to differences in the rate of hydrogen peroxide production (cf. Fig. S2 of the Supporting Information file). Obviously, these data support the applicability of the presently proposed system to real water matrices.

Finally, in order to complete the above analysis, the effect of the initial DCF concentration on the degradation rate has been studied also by HPLC and the results are shown in Fig. 11. As expected, there is some effect at short times but the final degradation fingerprint remains the same within experimental error.

4. Conclusions

The present work has shown that it is possible to construct an integrated device where hydrogen peroxide can be produced by using renewable resources and can be directly employed to degrade a recalcitrant organic pollutant. Hydrogen peroxide can be produced in a photocatalytic fuel cell which runs without any external bias and can operate simply by solar radiation. The photocatalytic fuel cell functioned in this work by using ethanol as fuel. Ethanol was used as model fuel for scientific research purposes but any biomass-derived byproduct or waste can be used in the place of ethanol thus providing an additional environmental benefit. A drawback of the present system is the necessity to employ an additional UV source. The cost of this extra component may be minimized by the employment of UV Light Emitting Diodes or even rely on solar UV itself. In this work, the pollutant was dissolved in the compartment where hydrogen peroxide was produced; however, a variant may be designed where the content of the reactor may be circulated with a pump so that exposure to solar UV may be facilitated. Although the environmental applicability of the proposed concept is demonstrated in this work and the basics are established by the present data, further research is required to optimize the process both in terms of kinetics and reactor setup; the in situ generation of oxidants, alongside the use of renewable sunlight are expected to (i) reduce overall treatment costs, and (ii) decouple reaction times from cost.

The photolysis of DCF creates a species with specific spectrophotometric characteristics and this allows the possibility to monitor the stage of degradation of DCF by UV–Vis spectroscopy provided that the pollutant concentration is high enough to be detectable by this method. This possibility is not offered by HPLC which can only monitor the degradation of the intact molecule. Therefore, the UV–Vis data introduced by the above measurements may be helpful in monitoring the process of DCF degradation, including mineralization. The latter can qualitatively be assessed through spectral changes occurring during the course of the reaction.

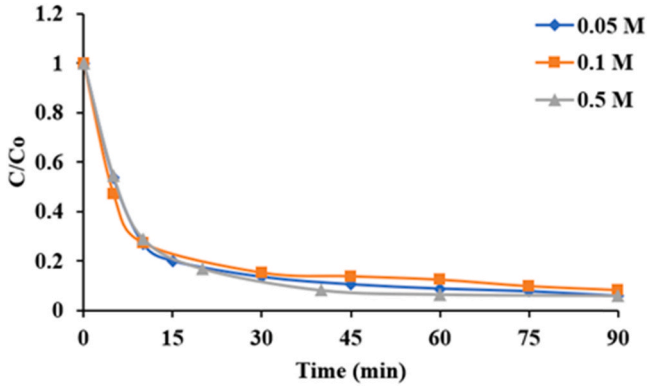

Fig. 9. HPLC measurements of the UV/H_2O_2 degradation of 2 μM DCF in the cathode compartment of a PFC at various Na_2SO_4 concentrations.

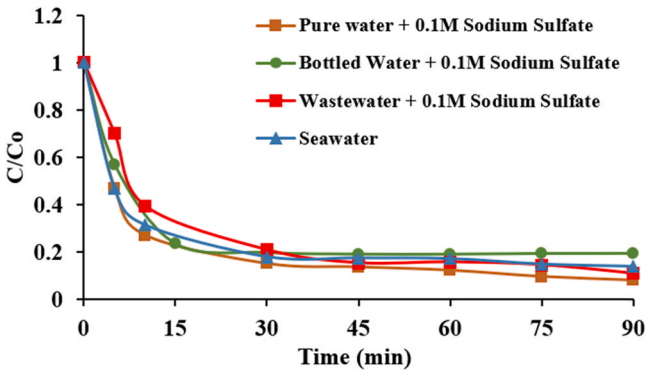

Fig. 10. HPLC measurements of the UV/H_2O_2 degradation of 2 μM DCF for four different cases of electrolytes introduced in the cathode compartment of the PFC, including pure, bottle, municipal waste and natural sea water.

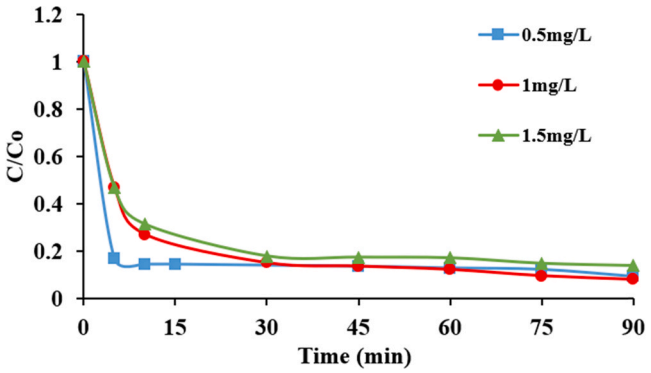

Fig. 11. Effect of DCF initial concentration on the UV/H_2O_2 degradation of the drug in the cathode compartment of the PFC.

CRediT authorship contribution statement

Rebecca Dhawle: Investigation. **Dionissios Mantzavinos:** Supervision. **Panagiotis Lianos:** Conceptualization.

Declaration of Competing Interest

The authors declare that they have no known competing financial interests or personal relationships that could have appeared to influence the work reported in this paper.

Acknowledgements

The authors are indebted to Dr. A. Petala for her help with actinometry measurements. This project has received funding from the European Union's EU Framework Programme for Research and Innovation Horizon 2020 under Grant Agreement No 861369 (innoveox.eu).

Appendix A. Supporting information

Supplementary data associated with this article can be found in the online version at doi:10.1016/j.apcatb.2021.120706.

References

[1] B.A. Wols, C.H.M. Hofman-Caris, Review of photochemical reaction constants of organic micropollutants required for UV advanced oxidation processes in water, Water Res. 46 (2012) 2815–2827, https://doi.org/10.1016/j.watres.2012.03.036.
[2] B.A. Wols, C.H.M. Hofman-Caris, D.J.H. Harmsen, E.F. Beerendonk, Degradation of 40 selected pharmaceuticals by UV/H_2O_2, Water Res. 47 (2013) 5876–5888, https://doi.org/10.1016/j.watres.2013.07.008.
[3] A.L. Garcia-Costa, A. Alves, L.M. Madeira, M.S.F. Santos, Oxidation processes for cytostatic drugs elimination in aqueous phase: a critical review, J. Environ. Chem. Eng. 9 (2021), 104709, https://doi.org/10.1016/j.jece.2020.104709.
[4] X. Lei, Y. Lei, X. Zhang, X. Yang, Treating disinfection byproducts with UV or solar irradiation and in UV advanced oxidation processes: a review, J. Hazard. Mater. 408 (2021), 124435, https://doi.org/10.1016/j.jhazmat.2020.124435.
[5] V.-D. Nguyen, X. Pierens, K. Benhabib, Experimental and numerical study of methylparaben decomposition in aqueous solution using the UV/H_2O_2 process, J. Environ. Sci. Health B 54 (2019) 357–365, https://doi.org/10.1080/03601234.2019.1571365.
[6] V.K. Sharma, X. Yu, T.J. McDonald, C. Jinadatha, D.D. Dionysiou, M. Feng, Elimination of antibiotic resistance genes and control of horizontal transfer risk by UV-based treatment of drinking water: a mini review, Front. Environ. Sci. Eng. 13 (2019) 37, https://doi.org/10.1007/s11783-019-1122-7.
[7] W.-L. Wang, Q.-Y. Wu, N. Huang, Z.-B. Xu, M.-Y. Lee, H.-Y. Hu, Potential risks from UV/H_2O_2 oxidation and UV photocatalysis: a review of toxic, assimilable, and sensory-unpleasant transformation products, Water Res. 141 (2018) 109–125, https://doi.org/10.1016/j.watres.2018.05.005.
[8] D.B. Miklos, C. Remy, M. Jekel, K.G. Linden, J.E. Drewes, U. Hübner, Evaluation of advanced oxidation processes for water and wastewater treatment – a critical review, Water Res. 139 (2018) 118–131, https://doi.org/10.1016/j.watres.2018.03.042.
[9] M.H.F. Graumans, W.F.L.M. Hoeben, M.F.P. van Dael, R.B.M. Anzion, F.G. M. Russel, P.T.J. Scheepers, Thermal plasma activation and UV/H_2O_2 oxidative degradation of pharmaceutical residues, Environ. Res. 195 (2021), 110884, https://doi.org/10.1016/j.envres.2021.110884.
[10] K. Guo, Z. Wu, S. Yan, B. Yao, W. Song, Z. Hua, X. Zhang, X. Kong, X. Li, J. Fang, Comparison of the UV/chlorine and UV/H_2O_2 processes in the degradation of PPCPs in simulated drinking water and wastewater: kinetics, radical mechanism and energy requirements, Water Res. 147 (2018) 184–194, https://doi.org/10.1016/j.watres.2018.08.048.
[11] P. Lianos, Review of recent trends in photoelectrocatalytic conversion of solar energy to electricity and hydrogen, Appl. Catal. B: Environ. 210 (2017) 235–254, https://doi.org/10.1016/j.apcatb.2017.03.067.
[12] T.S. Andrade, V. Dracopoulos, A. Keramidas, M.C. Pereira, P. Lianos, Charging a vanadium redox battery with a photo(catalytic) fuel cell, Sol. Energy Mater. Sol. Cells 221 (2021), 110889, https://doi.org/10.1016/j.solmat.2020.110889.
[13] T. Santos Andrade, I. Papagiannis, V. Dracopoulos, M. César Pereira, P. Lianos, Visible-light activated titania and its application to photoelectrocatalytic hydrogen peroxide production, Materials 12 (2019) 4238, https://doi.org/10.3390/ma12244238.
[14] H. Feng, M. Chen, R. Chen, X. Zhu, Q. Liao, D. Ye, B. Zhang, L. An, Y. Yu, W. Zhang, Anion-exchange membrane electrode assembled photoelectrochemical cell with a visible light responsive photoanode for simultaneously treating wastewater and generating electricity, Ind. Eng. Chem. Res. 59 (2020) 137–145, https://doi.org/10.1021/acs.iecr.9b06146.
[15] J. Zhang, J. Zheng, W. Yang, Green supercapacitor assisted photocatalytic fuel cell system for sustainable hydrogen production, Chem. Eng. J. 403 (2021), 126368, https://doi.org/10.1016/j.cej.2020.126368.
[16] Y. Vasseghian, A. Khataee, E.-N. Dragoi, M. Moradi, S. Nabavifard, G. Oliveri Conti, A. Mousavi Khaneghah, Pollutants degradation and power generation by photocatalytic fuel cells: a comprehensive review, Arab. J. Chem. 13 (2020) 8458–8480, https://doi.org/10.1016/j.arabjc.2020.07.016.
[17] R. Dhawle, Z. Frontistis, D. Mantzavinos, P. Lianos, Production of hydrogen peroxide with a photocatalytic fuel cell and its application to UV/H_2O_2 degradation of dyes, Chem. Eng. J. Adv. 6 (2021), 100109, https://doi.org/10.1016/j.ceja.2021.100109.
[18] X. Shi, Y. Zhang, S. Siahrostami, X. Zheng, Light-driven $BiVO_4$–C fuel cell with simultaneous production of H_2O_2, Adv. Energy Mater. 8 (2018), 1801158, https://doi.org/10.1002/aenm.201801158.
[19] K. Xiao, H. Liang, S. Chen, B. Yang, J. Zhang, J. Li, Enhanced photoelectrocatalytic degradation of bisphenol A and simultaneous production of hydrogen peroxide in saline wastewater treatment, Chemosphere 222 (2019) 141–148, https://doi.org/10.1016/j.chemosphere.2019.01.109.
[20] I. Papagiannis, E. Doukas, A. Kalarakis, G. Avgouropoulos, P. Lianos, Photoelectrocatalytic H_2 and H_2O_2 production using visible-light-absorbing photoanodes, Catalysts 9 (2019) 243, https://doi.org/10.3390/catal9030243.
[21] M. Antoniadou, P. Lianos, Near ultraviolet and visible light photoelectrochemical degradation of organic substances producing electricity and hydrogen, J. Photochem. Photobiol. A 204 (2009) 69–74, https://doi.org/10.1016/j.jphotochem.2009.02.001.
[22] D. Raptis, V. Dracopoulos, P. Lianos, Renewable energy production by photoelectrochemical oxidation of organic wastes using WO_3 photoanodes, J. Hazard. Mater. 333 (2017) 259–264, https://doi.org/10.1016/j.jhazmat.2017.03.044.
[23] P. Sathishkumar, R.A.A. Meena, T. Palanisami, V. Ashokkumar, T. Palvannan, F. L. Gu, Occurrence, interactive effects and ecological risk of diclofenac in environmental compartments and biota - a review, Sci. Total Environ. 698 (2020), 134057, https://doi.org/10.1016/j.scitotenv.2019.134057.
[24] L. Lonappan, S.K. Brar, R.K. Das, M. Verma, R.Y. Surampalli, Diclofenac and its transformation products: environmental occurrence and toxicity – a review, Environ. Int. 96 (2016) 127–138, https://doi.org/10.1016/j.envint.2016.09.014.
[25] B. Bonnefille, E. Gomez, F. Courant, A. Escande, H. Fenet, Diclofenac in the marine environment: a review of its occurrence and effects, Mar. Pollut. Bull. 131 (2018) 496–506, https://doi.org/10.1016/j.marpolbul.2018.04.053.
[26] A. Agüera, L.A.P. Estrada, I. Ferrer, E.M. Thurman, S. Malato, A.R. Fernández-Alba, Application of time-of-flight mass spectrometry to the analysis of phototransformation products of diclofenac in water under natural sunlight, J. Mass Spectrom. 40 (2005) 908–915, https://doi.org/10.1002/jms.867.
[27] K.A.K. Musa, L.A. Eriksson, Photodegradation mechanism of the common non-steroid anti-inflammatory drug diclofenac and its carbazole photoproduct, Phys. Chem. Chem. Phys. 11 (2009) 4601–4610, https://doi.org/10.1039/B900144A.
[28] J. Eriksson, J. Svanfelt, L. Kronberg, A photochemical study of diclofenac and its major transformation products, Photochem. Photobiol. 86 (2010) 528–532, https://doi.org/10.1111/j.1751-1097.2009.00703.
[29] S.K. Alharbi, J. Kang, L.D. Nghiem, J.P. van de Merwe, F.D.L. Leusch, W.E. Price, Photolysis and UV/H_2O_2 of diclofenac, sulfamethoxazole, carbamazepine, and trimethoprim: identification of their major degradation products by ESI–LC–MS and assessment of the toxicity of reaction mixtures, Process Saf. Environ. Prot. 112 (2017) 222–234, https://doi.org/10.1016/j.psep.2017.07.015.
[30] K. Fischer, S. Sydow, J. Griebel, S. Naumov, C. Elsner, I. Thomas, A. Abdul Latif, A. Schulze, Enhanced removal and toxicity decline of diclofenac by combining UVA treatment and adsorption of photoproducts to polyvinylidene difluoride, Polymers 12 (2020) 2340, https://doi.org/10.3390/polym12102340.
[31] Y. Huang, M. Kong, S. Coffin, K.H. Cochran, D.C. Westerman, D. Schlenk, S. D. Richardson, L. Lei, D.D. Dionysiou, Degradation of contaminants of emerging concern by UV/H_2O_2 for water reuse: kinetics, mechanisms, and cytotoxicity analysis, Water Res. 174 (2020), 115587, https://doi.org/10.1016/j.watres.2020.115587.
[32] M. Kovacic, N. Kopcic, H. Kusic, U.L. Stangar, D.D. Dionysiou, A.L. Bozic, Reactivation and reuse of TiO_2-SnS_2 composite catalyst for solar-driven water treatment, Environ. Sci. Pollut. Res. 25 (2018) 2538–2551, https://doi.org/10.1007/s11356-017-0667-x.
[33] M. Kovačić, K. Perović, J. Papac, A. Tomić, L. Matoh, B. Žener, T. Brodar, I. Capan, A.K. Surca, H. Kušić, U.L. Štangar, One-pot synthesis of sulfur-doped TiO2/reduced graphene oxide composite (S-TiO2/rGO) with improved photocatalytic activity for the removal of diclofenac from water, Materials 13 (2020) 1621, https://doi.org/10.3390/ma13071621.
[34] A. Al-Anazi, W.H. Abdelraheem, K. Scheckel, M.N. Nadagouda, K. O'Shea, D. D. Dionysiou, Novel franklinite-like synthetic zinc-ferrite redox nanomaterial: synthesis, and evaluation for degradation of diclofenac in water, Appl. Catal. B 275 (2020), 119098, https://doi.org/10.1016/j.apcatb.2020.119098.
[35] S.K. Alharbi, W.E. Price, Degradation and fate of pharmaceutically active contaminants by advanced oxidation processes, Curr. Pollut. Rep. 3 (2017) 268–280, https://doi.org/10.1007/s40726-017-0072-6.
[36] A. Ofrydopoulou, E. Evgenidou, Ch Nannou, M.I. Vasquez, D. Lambropoulou, Exploring the phototransformation and assessing the in vitro and in silico toxicity of a mixture of pharmaceuticals susceptible to photolysis, Sci. Total Environ. 756 (2021), 144079, https://doi.org/10.1016/j.scitotenv.2020.144079.
[37] D. Martínez-Pachón, R.A. Echeverry-Gallego, E.A. Serna-Galvis, J.M. Villarreal, A. M. Botero-Coy, F. Hernández, R.A. Torres-Palma, A. Moncayo-Lasso, Treatment of wastewater effluents from Bogotá – Colombia by the photo-electro-Fenton process:

elimination of bacteria and pharmaceutical, Sci. Total Environ. 772 (2021), 144890, https://doi.org/10.1016/j.scitotenv.2020.144890.

[38] S. Dimitriadou, Z. Frontistis, A. Petala, G. Bampos, D. Mantzavinos, Carbocatalytic activation of persulfate for the removal of drug diclofenac from aqueous matrices, Catalysis Today 355 (2020) 937–944, https://doi.org/10.1016/j.cattod.2019.02.025.

[39] W. Wu, S. Shabhag, J. Chang, A. Rutt, J.F. Whitacre, Relating electrolyte concentration to performance and stability for NaTi2(PO4)3/Na0.44MnO2 aqueous sodium-ion batteries, J. Electrochem. Soc. 162 (2015) A803–A808, https://doi.org/10.1149/2.0121506jes.